

A nonlinear model for soft rock and its application in bridge pier settlement calculation

M.S. Islam¹, M.S.A. Siddiquee^{1*}, F. Tatsuoka²

¹*Department of Civil Engineering
Bangladesh University of Engineering and Technology, Dhaka 1000, Bangladesh*
²*Tokyo University of Science, Noda shi, Chiba, Japan*

Abstract

A phenomenological model has been developed for soft rock based on the results of a series of triaxial compression (TC) tests conducted on Kobe sandstone with a very high measurement precision. From the analysis and interpretation of the test results, it has been found that small strain Young's modulus (E^s) is a function of the major principal stress. E^s for elastic strains of soft rock is assumed to be cross-anisotropic. A damage function has been used to derive the appropriate elastic Young's modulus when subjected to shear loading. As the basic stress-strain relation, the relationship between the tangent modulus and the shear stress level is used. The differential form of which is subsequently integrated by a 4th order Runge-Kutta solver to obtain the stress-strain relation. The model of soft rock considered an isotropic hardening elasto-plastic FEM solver which takes into account the pressure sensitivity, cross-anisotropy, degradation of Young's modulus with the degree of mobilized shear stress and the nonlinearity of the shear stress-shear strain relationship. This model is successfully calibrated with Akashi gravel and applied in the simulation for the settlement of Akashi-Kaikyo bridge piers. The simulations were carried out for both drained and undrained condition by changing the Poisson's ratio. The layering informations beneath the foundations were used in the FEM simulation. The use of very accurate Young's modulus from the field shear wave velocity test was the key to the successful simulation of the settlement under bridge pier foundations.

Keywords: FEM, model, soft rock and simulation.

1. Introduction

In recent years, since increasing number of foundations have been placed on soft rock, it becomes of great importance to evaluate mechanical properties of soft rocks accurately. General aspects and engineering characteristics of soft rocks in Japan were reported by different researchers such as Aki et al. (1979). Numerous failure criteria for foundation

** Email: sid@ce.buet.ac.bd

satiability analyses or elastic-plastic finite element analyses have also been proposed. As concerns relationships between the confining pressure and strength of soft rocks, power function models were proposed by Hobbs (1966), Yoshinaka and Yamabe (1980) and Adachi and Ogawa (1980). It is reasonable that linear equations such as the Mohr-Coulomb's failure criterion are not suitable for soft rocks. But instead, non-linear equations as a power function may better describe the failure model for soft rocks. In this context, a general methodology for modelling the stress-strain relationship for soft rock has been developed.

The modeling has been carried out by mathematical formulation of the stress-strain relations obtained by a long-term element test programme at the Institute of Industrial Science (IIS), University of Tokyo, Japan. (Hayano et al., 1997; Jiang et al., 1998; Kohata et al., 1997, Tatsuoka and Kohata, 1995; Tatsuoka and Kim, 1995 and Tatsuoka et al., 1995). The model is derived from the laboratory triaxial compression (TC) test results. All the tests were equipped with Local Deformation Transducers (LDT) to obtain stress-strain relations at small strains free from the effect of bedding error (Goto et al., 1999). Elastic deformation parameters, the Young's modulus, were obtained from small unloading-reloading cycles applied during the TC testing. The model considers the pressure level-dependency of elastic Young's modulus, stress system-induced anisotropy, non-linearity of stress-strain relations, damage to micro-structures by shearing while based on field Young's modulus (E_f) from in-situ shear wave velocity measurements. The mentioned soft rock model is developed basically from the TC test data of Kobe sandstone. Finite Element Method (FEM) is used to simulate the settlement under the pier foundations of Akashi-Kaikyo Bridge. During the FEM simulation of the settlement of the pier 2P, of the Akashi-Kaikyo Bridge in Japan, it was found that there is a layer of Akashi-gravel at the top. However, available TC test data for Akashi gravel was limited. In the absence of availability of adequate test data on Akashi gravel, the soft rock model developed in this study is calibrated for the Akashi gravel to simulate the pier 2P's behaviour with layering information. This paper deals with the development of the model for the particular soft rock. Application of this model to simulate the settlements of the pier of the Akashi-Kaikyo Bridge in Japan has been presented.

2. Properties of Akashi sandstone

Wet density of the Akashi sandstone ranges from 1.99 to 2.19 g/cm³ with an average value of 2.09 g/cm³ (Kashima et al., 1995). The measured wet density is smaller than the actual density because of water loss in the samples during sampling. The calculated saturated density varies in a small range from 2.10 to 2.20 g/cm³ as compared to the wet density. Grain size distributions of this sand are also available in Kashima et al. (1995). The maximum diameter (D_{max}) ranges from 36 to 136 mm and a diameter at 60% finer (D_{60}) ranges from 0.70 to 19.00 mm. The Akashi sandstone is mostly classified into gravel with fines based on Japanese Soil Classification. The coefficient of uniformity generally exceeds 10. Gravel shape is mainly subangular and subrounded. The formation contains 20 to 30% of decomposed gravel.

3. Constitutive model

An elasto-plastic isotropic hardening model is employed here for the soft rock. The plastic part is modeled by a non-associated flow rule based on a generalized Mohr-Coulomb yield function along with a Drucker-Prager type plastic potential function. As the basic stress-strain relation, the relationship between the tangent shear modulus and the

shear stress level is used (hence called “plasticity function”), the differential form of which is subsequently integrated by a 4th order Runge-Kutta solver to obtain the stress-strain relation. A damage function is used to describe the degradation of Young’s modulus due to micro-cracking that develops with the increase in shear stress. However, unlike the constitutive relations for sand, the constitutive relations for soft rock does not include softening, shear banding and strength anisotropy. The model traces the stress-strain relation up to the peak.

3.1 Young’s modulus

From the triaxial compression (TC) test results (Hayano et. al., 1997; Jiang and Kohata, 1998; Jiang et al., 1998; Kohata et al., 1997), it has been observed that small strain Young’s modulus (E^e) for elastic major principal strain is a function of the major principal stress, i.e., $E^e = f(\sigma_1)$. Figure 1 shows the variation of E_{\max} ($=E^e$) with confining pressure (σ_j) for Kobe sandstone. It is seen that E_{\max} increases with the increase of σ_1 . The plot also shows an apparent linear relation signifying a power law dependence of E^e on σ_1 . In Figure 1, E_0^e is the value of Young’s Modulus at zero confining pressure.

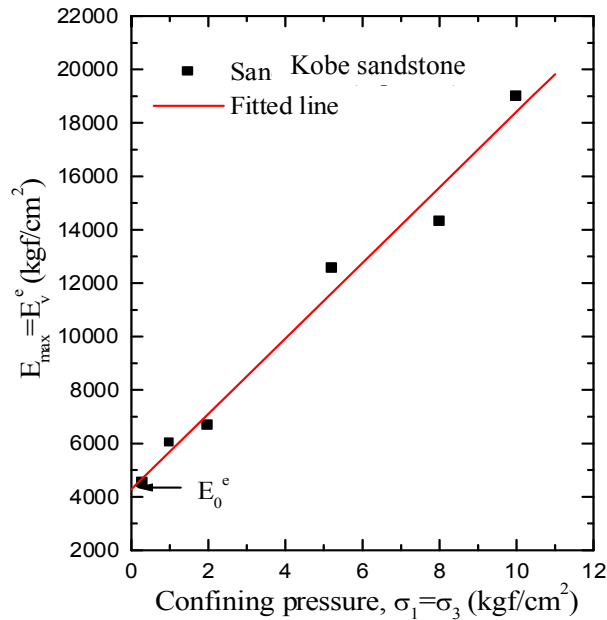


Fig. 1. Variation of $E_{\max}(E^e)$ with $\sigma_1 = \sigma_3$.

3.2 Cross-anisotropy

The Young's modulus E^e for elastic strains of soft rock is assumed to be cross-anisotropic. From the test results it was seen that the Young's modulus, E^e for elastic strains of Kobe sandstone can be reasonably assumed to be cross-anisotropic (Hoque and Tatsuoka, 1998) under axially symmetric stress conditions (stress system-induced anisotropy). This feature is modeled as described in Eq. 1.

$$E_v^e = E_0^e + a\sigma_v^b, \quad E_h^e = E_0^e + a\sigma_h^b \quad (1)$$

where, E_v^e and E_h^e are the Young's moduli for elastic normal strains in the vertical and horizontal directions, respectively. E_0^e is the value of Young's modulus at zero confining pressure (Fig. 1).

As the material has a cohesion, E_0^e is a non-zero value. From Eq. (1), $E_v^e = E_h^e = E_0^e$ is obtained when $\sigma_v = \sigma_h$, namely inherent isotropy is assumed for elasticity. From the energy conservation law, the following relationships are obtained;

$$\nu_{hv}^e = \nu_0^e \alpha, \quad \nu_{vh}^e = \nu_0^e \alpha^{-1} \quad (2)$$

where, $\alpha = \sqrt{E_h^e / E_v^e}$, ν_{hv}^e = Poisson's ratio for the deformation from horizontal to vertical directions (vice versa for ν_{vh}) and ν_0^e is the Poisson's ratio for elastic strains under isotropic stress conditions. In the same way, the shear modulus G_{hv}^e for elastic shear strains is derived as described in Eq. 3.

$$G_{hv}^e = E_{45}^e / 2(1 + \nu_0^e)$$

$$E_{45}^e = E_0^e + a\{0.5(\sigma_v + \sigma_h)\}^b \quad (3)$$

where, G_{hv}^e is cross anisotropic shear modulus in $h \sim v$ plane and E_{45}^e is cross anisotropic Young's modulus at an angle 45° with $h \sim v$ plane. E_0^e is isotropic Young's modulus, σ_v is current vertical stress component and σ_h is current horizontal stress component, respectively. E_{45}^e is E^e when the direction of σ_1 is at 45° relative to the vertical.

3.3 Damage function

The concept of the damage function is developed due to the experimental evidence of the deterioration of the material strength, reflected in the continuous reduction of equivalent Young's modulus E^e when compared to E_{max} under an identical σ_1 , depending on the amplitude of shear stress. The evaluation of the damage function was necessary for the following two cases.

3.3.1 Elastic modulus

An empirical model was developed for the Kobe sandstone based on the results for consolidated drained triaxial compression (TC) tests measuring axial strain locally. The core samples tested were obtained by block sampling from the bottom of the excavation to a depth of 61 m for pier 1A of Akashi-Kaikyo Bridge (Kohata et al., 1994).

At a depth of 61m, four plate loading tests using a rigid 60 cm-diameter plate were performed. Figure 2 shows the variation of different Young's Moduli with depth. The initial Young's moduli, E_{max} defined at axial strains less than about 0.001 % in the TC tests performed at an confining pressure equal to the original in-situ effective over-

burden pressure are only slightly smaller than the Young's moduli E_f from field shear wave velocities. The difference is due partly to the drained condition in the TC tests compared to the undrained condition in the seismic survey (thus by the factor of $(1+0.2)/(1+0.46)$, in which 0.2 and 0.46 are drained and undrained Poisson's ratios, respectively). The difference is also due partly to the effects of inevitable sample disturbance.

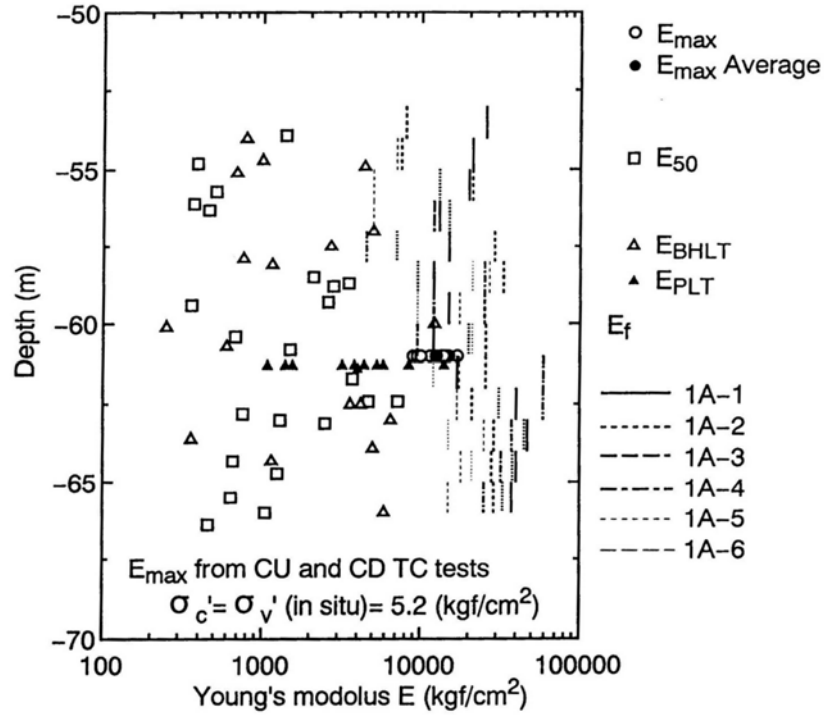


Fig. 2. Variation of Young's moduli with depth (E_f : from shear wave velocity measurements, E_{max} from local axial strains by LDT, E_{50} from unconfined compression tests with external axial strains, E_{BHLT} : from bore hole loading test, E_{PLT} : from plate loading test).

As also presented in Kohata et al. (1994), the Young's modulus, E_{eq} for elastic axial strains measured in small unload/reload cycles during triaxial compression is primarily a function of the axial stress σ_1 , exhibiting cross-anisotropy. However, with shearing E_{eq} becomes noticeably smaller than E_{max} ($=E_v^e$ under isotropic stress conditions) measured at the same axial stress (σ_1). The variation of equivalent Young's modulus determined from the slope of the unloading-reloading curve E_{eq} and maximum Young's modulus obtained from the beginning part of the shearing by monotonic loading, E_{max} for the same σ_1 is plotted in Figure 3. In this Figure, m is defined as stated in Eq. 4.

$$\frac{E_{eq}}{E_{max}} = E_0^e + a\sigma_1^m \quad (4)$$

Comparing Eq. 1 and 4, we can find that $m = b$. Figure 3 describes the relationships between E_{max} , E_{eq} and σ_1 for different m values i.e., 0, 0.5 and 0.7. In this figure, E_{max} is denoted as $E^e(\sigma_1)$. As this reduction in E_{eq} can be considered due to the damage to the micro-structure by shear deformation, the relation between the ratio $E_{eq}/E^e(\sigma_1)$ and the shear stress level q/q_{max} is defined as the damage function f_d^e as stated in Eq. 5.

$$E_{eq}(\sigma_1) = E^e(\sigma_1) \cdot f_d^e(\tau/\tau_{max}) \quad (5)$$

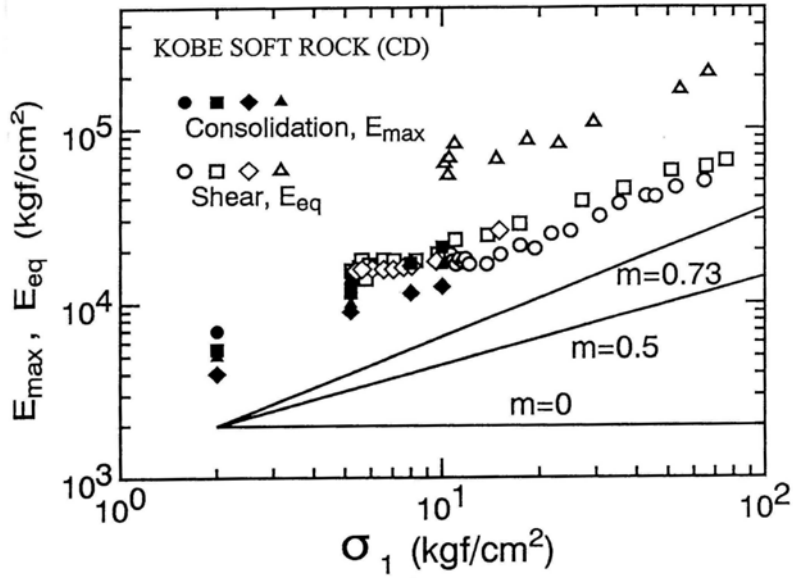


Fig. 3. Variation of E_{max} and E_{eq} with σ_1 .

where, E_{eq} is Equivalent Young's modulus determined from small amplitude cyclic-loading test, σ_1 is major principal stress and τ/τ_{max} is relative mobilized shear stress which is equal to q/q_{max} .

The variation of $E_{eq}/E^e(\sigma_1)$ with q/q_{max} for Akashi-gravel is presented in Figure 4. For the first approximation, the average relationship for E_{eq} and q/q_{max} can be modeled by a simple hyperbolic function as described in Eq. 6.

Function-1

$$f_d^e\left(\frac{\tau}{\tau_{max}}\right) = \frac{1}{1 + 2.75 \cdot (\tau/\tau_{max})} \quad (6)$$

The average relation can be also modeled more precisely by the following Eq. 7.

Function-2

$$\left. \begin{aligned} (\tau/\tau_{\max}) \leq 0.137, \quad f_d^e\left(\frac{\tau}{\tau_{\max}}\right) &= \frac{1 - 0.15 * (\tau/\tau_{\max})^{0.15}}{1 + (\tau/\tau_{\max})^{0.25}} \\ (\tau/\tau_{\max}) > 0.137, \quad f_d^e\left(\frac{\tau}{\tau_{\max}}\right) &= 0.5519 \end{aligned} \right\} \quad (7)$$

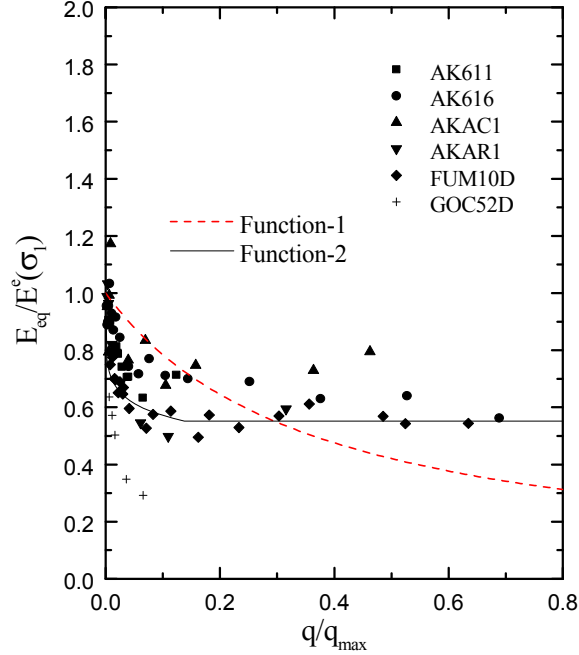


Fig. 4. Decrease in E_{eq} with shear stress level (Akashi sandstone).

For the model, the relationship between $E^e(\sigma_1)$ and τ_{max} was obtained by averaging the TC test results. These relationships are described in Eq. 8.

$$\begin{aligned} E_{\max} &= 4276.28 + 1413.56\sigma_1 \\ \tau_{\max} &= 39.03 + 1.33\sigma_3 \end{aligned} \quad (8)$$

in which E^e , τ_{max} , σ_1 and σ_3 are in kgf/cm^2 . The damaged shear modulus G_{eq} for elastic strains is obtained as $E_{eq}(\sigma_1)/\{2(1 + \nu^e)\}$, in which ν^e is the Poisson's ratio for elastic strains assumed to be equal to 0.2 and 0.46 for drained and undrained conditions, respectively.

3.3.2 Plasticity function

For the undrained TC tests, the tangent shear modulus G_{tan} can be obtained from the relationship between the deviator stress and the locally measuring axial strain, since the shear strain, γ is obtained as $\gamma = (3/2)\varepsilon_1$. On the other hand, for the drained TC tests, the available raw data of the drained TC tests are locally and externally measured axial

strains, and externally measured volumetric strains obtained from the amount of the pore water expelled from or soaked into a specimen. So the bedding error was first determined in the axial direction, i.e., ε_1 as a function of σ_1 . The same amount of correction for ε_1 was applied to the recorded volumetric strain, ε_v , as a correction factor for the calculation of radial strain in order to determine the maximum shear strain, i.e.,

$$\text{Correct } \gamma = (\varepsilon_1)_{\text{locally measured}} - (\varepsilon_3)_{\text{corrected}} \quad (9)$$

where,

$$(\varepsilon_3)_{\text{corrected}} = \frac{3}{2}(\varepsilon_1)_{\text{locally measured}} - \frac{1}{2}(\varepsilon_v)_{\text{corrected}}$$

$$(\varepsilon_v)_{\text{corrected}} = (\varepsilon_v)_{\text{measured}} - \{(\Delta\varepsilon_1)_{\text{BE}} \text{ as a function of } \sigma_1\}$$

This shear strain is used to calculate G_{tan} from the results of the undrained TC tests. The value of G_{tan} for ε_1 in the vertical direction is normalized by respective G_{max} (calculated from the experimental Young's modulus, $E^e(\sigma_1)$ and an assumed Poisson's ratio of 0.2 for drained tests and 0.46 for the undrained tests, respectively). The tangent shear modulus G_{tan} for total shear strains measured during the TC tests on Akashi sandstone divided by $G^e(\sigma_1) = E^e / \{2(1 + \nu^e)\}$ are plotted against q/q_{max} in Figure 5.

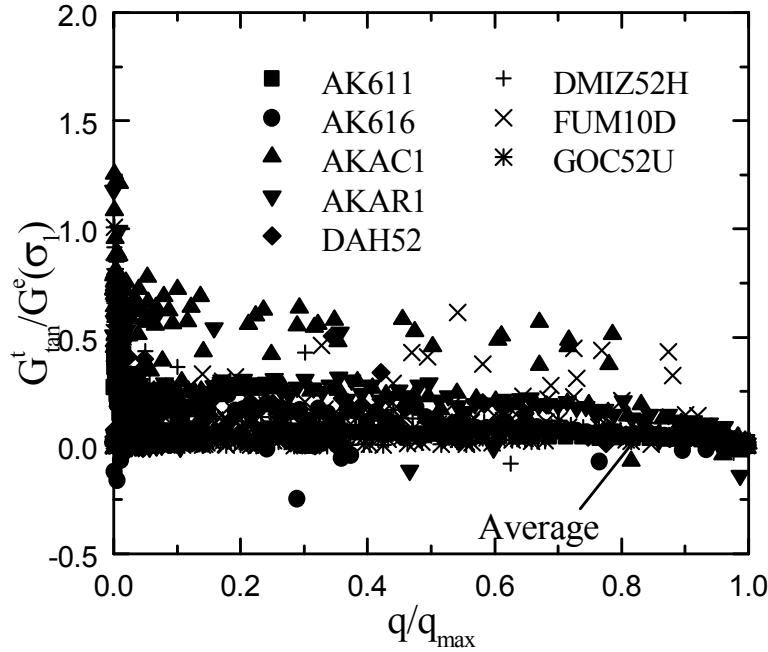


Fig. 5. $G_{tan}^t / G^e(\sigma)$ versus q/q_{max} (Akashi sandstone).

Here, in choosing the plasticity function that it was the function that starts from 1.0 when q/q_{max} is 0 and it is 0.0 when q/q_{max} is 1.0. It is seen from the Figure 5 that the function drops sharply at the beginning, followed by a flat part, which characterizes a S-shape stress-strain curve. This trend is believed to be linked to such a physical meaning as the opening of the micro cracks due to the initial shear loading stage. Subsequently,

the ratio, $G_{tan}/G^e(\sigma_1)$ rises a little and again drops towards zero as q/q_{max} approaches 1.0. A systematic difference between the drained and undrained conditions was not found. To express the peculiar behavior that the ratio decreases very sharply with q/q_{max} at the initial stage followed by a slight increase and a subsequent gradual decrease to zero, the following Eq. (10) was chosen, while the parameters were obtained by non-linear regression of the data.

$$G_{tan}^t(\sigma_1) = G^e(\sigma_1) \cdot h^s(\tau/\tau_{max}) \quad (10)$$

$$h^s(y) = \frac{1 - y + c(y^2 - y) + d(y^3 - y)}{1 + by} \quad (11)$$

where, $y = \tau/\tau_{max}$, $b=9674$, $c=778$ and $d=-2740$. The plasticity function h^s is equal to the damage function for G_{eq} times the ratio "damaged elastic shear strain increment"/"total shear strain increment".

4. FEM implementation

In this research, classical non-associated elasto-plastic isotropically hardening non-linear Finite Element Method (FEM) is used. In order to capture the basic behaviour of soft rock, Mohr-Coulomb type of yield function and Druker-prager type of plastic potential is used. A four noded iso-parametric element was used with 1-point integration. The probable hour-glass mode was prevented (Flanagan and Belytschko, 1981). A highly optimized non-linear equation solver, Dynamic Relaxation (DR) (Tanaka and Kawamoto, 1988) is used to solve the nonlinear equations, resulting from the material nonlinearity. Integration of the elasto-plastic equations was performed by means of a return mapping scheme (Ortiz and Simo, 1986). Selectively reduced integration (reduced integration on shear terms) was used to reduce the shear locking near incompressible situation. Dilatency is implemented via modified Rowe's stress-dilatancy relation. General elasto-plastic frame work of the model is described below:

This is essentially an elasto-plastic isotropic strain hardened analysis with non-associated flow rule (Eq. 12).

$$\phi = \alpha I_1 + \frac{1}{g(\theta)} \sqrt{J_2} - K = 0 \quad (12)$$

$$\text{where, } g(\theta) = \frac{3 - \sin \phi_{mob}}{2\sqrt{3} \cos \theta - 2 \cos \theta \sin \phi_{mob}} \text{ and } \alpha = \frac{2 \sin \phi_{mob}}{\sqrt{3}(3 - \sin \phi_{mob})}$$

where, J_1 is 1st stress invariant, J_2 is 2nd invariant of deviatoric stress, K is cohesion terms, θ is Load angle, and ϕ_{mob} is mobilized angle of internal friction.

The original Rowe's stress-dilatancy relation was modified to define the plastic potential as stated in Eq. 13.

$$\psi = \alpha' I_1 + \sqrt{J_2} - K = 0 \quad (13)$$

where, $\alpha' = \frac{2 \sin \psi}{\sqrt{3(3 - \sin \psi)}}$, $\sin \psi = \frac{\sin \phi_{mob} - \sin \phi_r}{1 - \sin \phi_{mob} \sin \phi_r}$ and ϕ_{mob} is mobilized angle of internal friction and ψ is mobilized angle of dilatancy.

The evolution of the yield function is modeled as described in Eq. 14 (Tanaka and Kawamoto, 1988).

$$\alpha = \int (\kappa) \quad (14)$$

$$\text{where, } \kappa = \int d\varepsilon^P \text{ and } d\varepsilon^P = [2(de_{11}^P)^2 + 2(de_{22}^P)^2 + 2(de_{33}^P)^2 + (d\gamma_{11}^P)^2 + (d\gamma_{23}^P)^2 + (d\gamma_{31}^P)^2]^{1/2}$$

$de_{ij}^P \sim d\gamma_{ij}^P$ are the deviatoric components of plastic strain increments, κ = plasticity parameter (internal variable).

5. Verification of FEM formulation

The model thus developed in this study has been used to simulate the actual settlement measured under the piers of the Akashi-Kaikyo Bridge in Japan. Figure 6 shows the detail layout of the bridge. The bridge is for 6-lane highway with the design speed of 100 km/hr. On April 5, 1998, the Akashi-Kaikyo Bridge was completed and opened to traffic. The bridge, which links Kobe city and Awajshima Island both in Hyogo Prefecture, has main span of 1991 m and a total length of 3911 m and thus becomes the world's largest suspension bridge. The construction work of the bridge foundations has been finished successfully in 1993, which started 20 years before with an investigation of laying the foundation of bridge-pier and keeping it in-place against very strong sea current. The bridge rested on two huge anchors and other two pier foundations. The two middle piers were named as 2P and 3P. The caissons of the piers were constructed elsewhere and tugged by boats to the place of the bridge foundation. The places of the pier foundations were first excavated to some depth (15 to 20 m) and then the caissons were sunk by pouring water inside. Then the inside was filled by underwater concreting. Namely, first the outer chamber of the pier caisson is filled with concrete and then the main body was filled with concrete. The base rock beneath the straits is granite, on which Kobe formation (alternating layers of sand stone and mud-stone in the Miocene), Akashi formation (semi consolidated sand and gravel layer in the late Pliocene and the early Pleistocene) and the Alluvium layer are deposited.

5.1 Simulation using laboratory test data

The FEM simulation followed the sequence of excavation and concrete filling. Two series of analysis were performed. In the first series, the simulation was performed based on the model described in article 3, which has been calibrated only by the results of laboratory TC tests data of the undisturbed samples of sedimentary soft rock obtained at the site of anchor 1A, and those of Akashi gravel obtained at the site of Pier 2P. In the second series, another set of simulations were carried out by using the maximum Young's modulus obtained from field shear wave velocity in each layer.

At the pier 2P, there is a thin weak layer of Akashi gravel which is also modeled using the same approach as of the Kobe soft rock. Only a difference is the lack of the damage

function for the Young's modulus for the gravel. In the FEM simulation, the sequence of ground excavation and footing construction analysis was begun by removing all the elements to be excavated and then applying the self weights of concrete under sea water each by each layer while iterating the solution for equilibrium. Figure 7 shows the FEM idealization of the pier sites 2P and 3P. Figure 8 shows the meshes used for the analysis of 2P and 3P pier foundations.

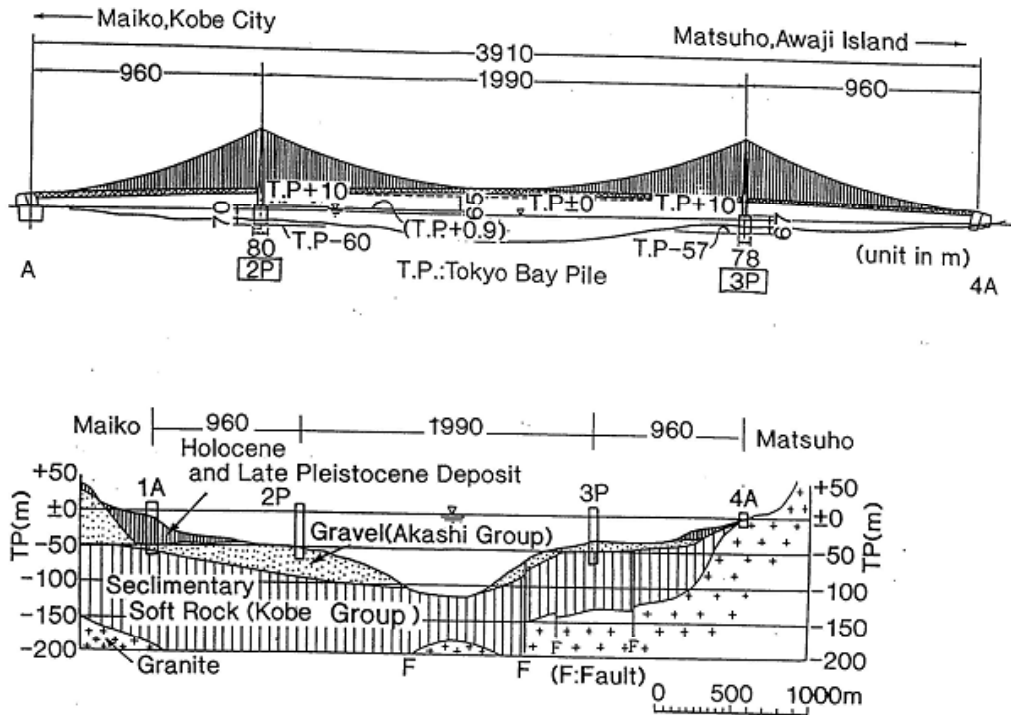


Fig. 6. Details layout of Akashi-Kaikyo Bridge piers.

The analysis was carried out under axisymmetric loading conditions. Figure 9 shows the simulated load-displacement curves for 2P and 3P pier foundations, which include the measured load-settlement curve. As it can be seen that the FEM simulations were done separately for two different conditions using (a) a drained Poisson's ratio, $\nu=0.2$ and (b) an Undrained Poisson's ratio, $\nu=0.46$. It can be observed from the Figure 9 that the measured load-settlement data lies close to the undrained solution. The comparison between the FEM simulation and the measured behavior suggests that the construction was not slow enough to allow fully drained conditions, and if the construction would have taken considerably long time, extra settlement due to consolidation would have resulted. In any case, it can be said that as a whole the simulated results were quite close to the measured data. Detail settlement profile are calculated at five load levels along the central line of the pier foundations as marked 1 to 5 on Figure 9. The details of the results are available in Siddiquee (1994).

5.2 Simulation using the field data

Below each of the two piers, there were several layers of the same material, which have different shear wave velocity values, i.e., different shear modulus values. This

information was used to determine the elastic Young's modulus as closely as possible to the field Young's modulus. This goal is attained by the following method. First, the overburden pressure, σ_{v0} at the central depth of each layer and its field Young's modulus, E_{f0} were obtained. Then using the equations for the Young's modulus variation found from TC tests data (Eq. 8), the elastic Young's modulus E^c was obtained as described in Eq. 15.

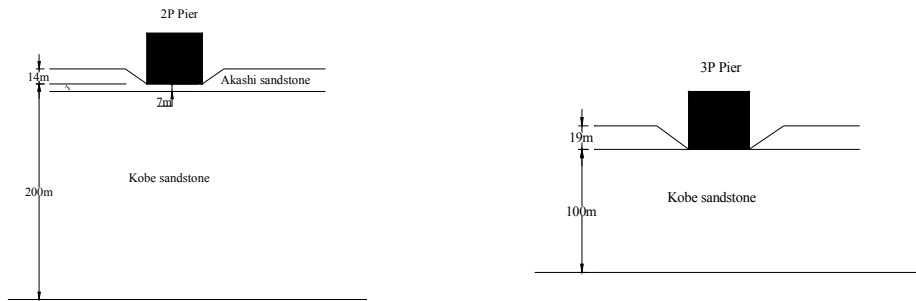


Fig. 7. FEM idealization of 2P and 3P pier site (using laboratory test data).

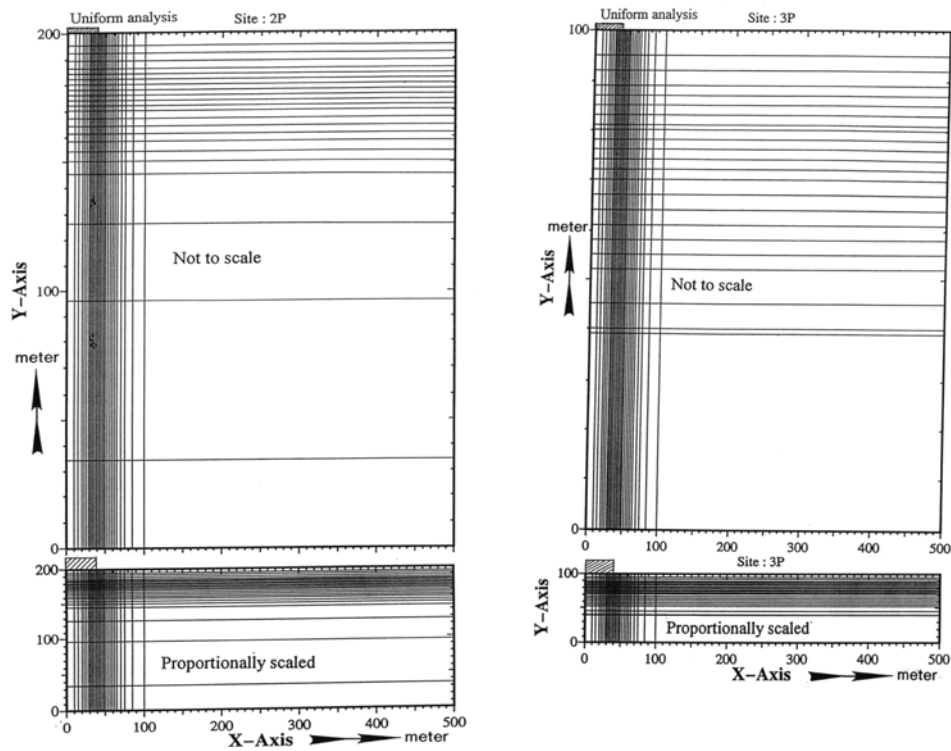


Fig. 8. Mesh used in the FEM simulation of settlement of Akashi-Kaikyo Bridge pier 2P and 3P.

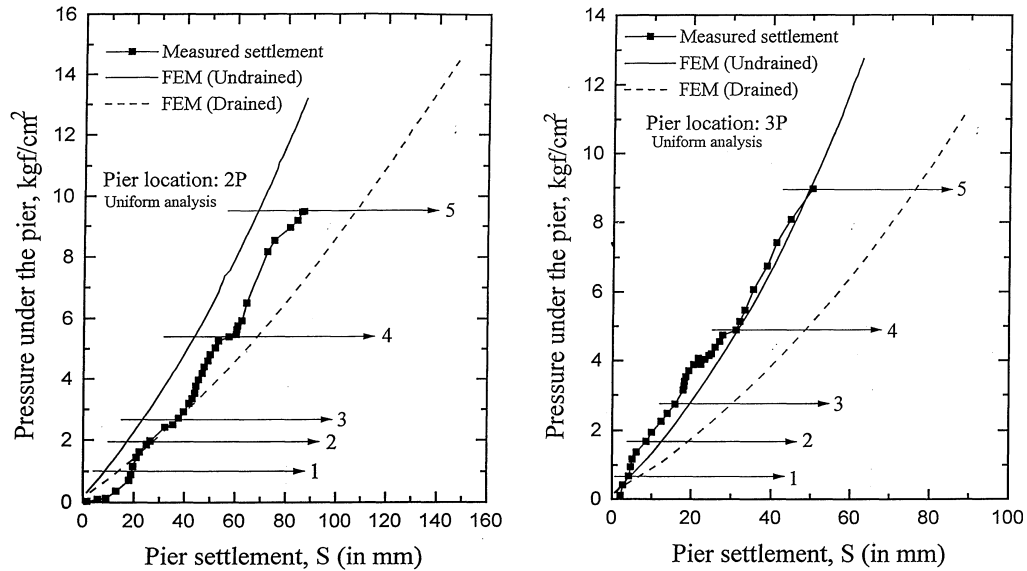


Fig. 9. Load-settlement curves of the Akashi-Kaikyo Bridge pier foundations 2P and 3P.

$$E^e = E_{f0} + \text{Constant} \cdot (\sigma_c - \sigma_{v0}) \quad (15)$$

where, E^e is elastic Young's modulus, E_{f0} is the Young's modulus at the top layer, σ_c is the confining stress at current layer and σ_{v0} is confining stress at top layer. In the above equation, the rate of the increase in the Young's modulus obtained from TC test data ("Constant" in Eq. 15) and the basic field Young's modulus E_{f0} from the field shear wave velocity data are used. The layering information at the pier 2P and 3P are provided in Figure 10 and Tables 1 and 2.

Table 1. Layer information for the pier 2P (depth of excavation = 14m)

Layer name	Layer thickness (m)	γ_{sat} (t/m^3)	V_s (m/s)	Poisson's ratio, ν	Calculated σ_{v0} (kgf/cm^2)	Calculated E_{f0} (kgf/cm^2)
A _k	7	1.96	360	0.47	0.651	2592.0
K _{2p-1}	32	2.15	450	0.44	3.360	4442.6
K _{2p-2}	28	2.27	720	0.44	6.840	12007.8
K _{2p-3}	30	2.24	710	0.43	10.770	11522.2
K _{2p-4}	62	2.28	880	0.43	16.870	18016.6
Gr ^r	34	2.35	1100	0.45	24.150	29015.3

In Tables 1 and 2 the layer thickness values are calculated from the bottom of each pier foundation. The diameter of the pier foundation is 80 m and 78 m for 2P and 3P, respectively. Figure 11 shows the FEM mesh used here in this layered soil analysis to accommodate the layers in such a way that the mesh size changes smoothly.

Figure 12 shows the simulated load-displacement curves (Siddique, 1995; Siddique et al., 1994 and 1995) for both 2P and 3P pier foundations containing the measured load-settlement data.

Table 2. Layer information for the pier 3P (depth of excavation = 19m)

Layer name	Layer thickness (m)	γ_{sat} (t/m ³)	V_s (m/s)	Poisson's ratio, ν	Calculated σ_{v0} (kgf/cm ²)	Calculated E_{f0} (kgf/cm ²)
K _{3p-2}	9	2.27	470	0.47	1.736	5111.7
K _{2p-3}	14	2.34	560	0.47	4.585	7488.0
K _{2p-4}	6	2.34	590	0.47	5.895	8311.0
K _{2p-5}	12	2.20	450	0.48	6.480	4545.9
K _{2p-6}	1	2.36	730	0.46	8.046	12833.1
Gr'	29	2.35	860	0.45	10.626	17735.3

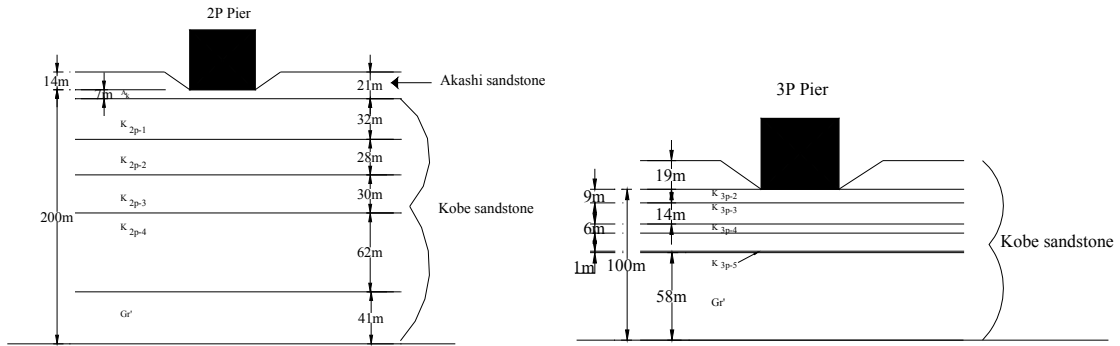


Fig.10. Layer information for the pier 2P and 3P as used in the FEM discretization.

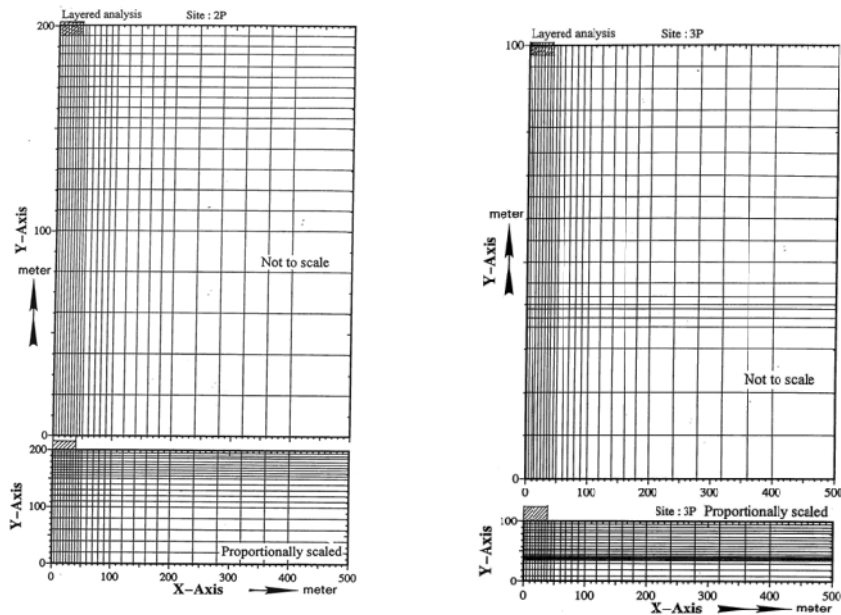


Fig. 11. Mesh used in the FEM simulation of settlement of Akashi-Kaikyo bridge pier 2P and 3P.

The simulations were performed for two drainage conditions varying the Poisson's ratio as (a) fully drained condition by applying a Poisson's ratio, $\nu=0.2$ and (b) fully undrained condition with a Poisson's ratio of $\nu=0.46$. The results are expected to be

stiffer than the previous simulation considering only the same models as to Young's modulus for each soil or rock type containing several layers. Because the shear modulus obtained from the shear wave velocity at these layers are in general greater than its corresponding values obtained at the stress values of layer mid height from the empirical equation for E_{max} versus σ_v based on the laboratory test data. But some of the layers at greater depths actually had values of shear modulus E_{f0} from the field seismic survey, which are lower than the values based on Eq. 8. This situation resulted in a relatively softer response in the simulation of 2P-pier foundation. Detail settlement profile are calculated at five load levels along the central line of the pier foundations as marked 1 to 5 on Figure 12. The details of the results are available in Siddiquee (1994).

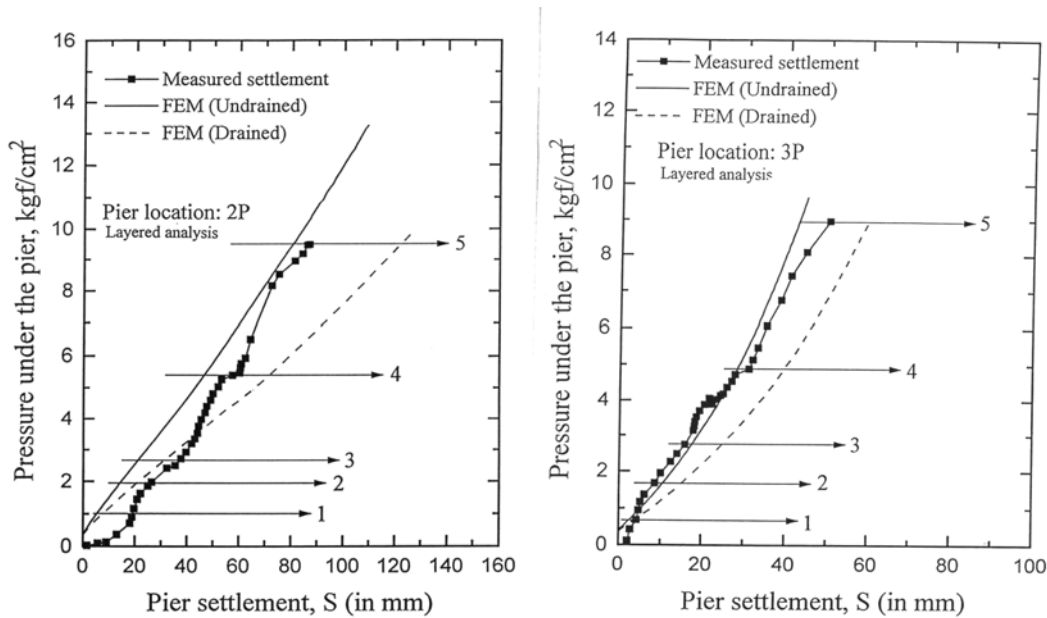


Fig. 12. Load-settlement curves of the Akashi-Kaikyo bridge pier foundation 2P and 3P.

6. Conclusions

A novel model has been developed for soft rock based on the laboratory test results. This model is successfully used for simulating the settlement of the bridge pier foundations. A continuum approach has been devised to model stiff geomaterials by masking the effect of micro-cracks through the introduction of a damage function. Pressure level dependency, cross anisotropy and nonlinearity contributed towards the realistic simulation of the load-settlement behavior of the Akashi-Kaikyo Bridge piers. It is shown that field seismic survey data can be used directly to model such materials as soft rock.

The small strain Young's modulus E^e is a function of the major and minor principal stresses. The small strain Young's modulus E^e of soft rock is assumed to be cross-anisotropic as interpreted from the TC test results. A damage function has been devised to derive the appropriate elastic Young's modulus when subjected to shear loading. The plasticity has been modelled by tangential Young's modulus/tangential shear modulus, whichever available. The tangential shear modulus is further decomposed into two

components. One part grows with major principal stress and another part decreases with increasing mobilized shear stress.

Settlement under the piers of the Akashi-Kaikyo Bridge has been simulated successfully using the developed model and the field modulus. The simulation of the settlement of the piers under drained and undrained condition has been carried out. It has been found that simulation in drained condition is closer to the actual settlement record.

References

- Adachi, T., Ogawa, T., 1980. Mechanical properties and failure criterion of soft sedimentary rock. *Journal of Geotechnical Engineering, JSCE* 295, 51-63 (in Japanese).
- Aki, K., Adachi, T., Nishi, K., 1979. Time dependent characteristics and constitutive equations of soft rock (porus tuff). *J. Geotec. Engg., JSCE* 282, 75-96 (in Japanese).
- Flanagan, D. P., Belytschko, T., 1981. A uniform strain hexahedron and quadrilateral with orthogonal hourglass control. *International Journal of Numerical Methods in Engineering* 17, 679-706.
- Goto, S., Burland, J. B., Tatsuoka, F., 1999. Non-linear soil model with various strain levels and its application to axisymmetric excavation problem. *Soils and Foundations* 39 (4), 111-119.
- Hayano, K., Sato, T., Tatsuoka, F., 1997. Deformation characteristics of a sedimentary softrock from triaxial compression tests using rectangular prism specimens. *Geotechnique*, 47 (3), 439-449.
- Hobbs, D.W., 1966. A study of behaviour of broken rock under triaxial compression and its application to Mine Roadways. *Int. J. Rock Mech., Mining Sci.* 3, 11-14.
- Hoque, E., and Tatsuoka, F. 1998. Anisotropy in the elastic deformation of materials. *Soils and Foundations* 38(1), 163-179.
- Jiang, G.L., Kohata, Y., Sunaga, M., 1998. Some factors affecting deformation characteristics at small strains of a sandy gravel. *Journal of Railway Technical Research Institute* 12 (4), 49-54 (in Japanese).
- Kashima, S., Yamamoto, S., Takahashi, M. Sasao, Yamada, S., 1995. Large scale sampling of Akashi gravelly layer and its mechanical property. *Rock Foundation, Yoshinaka & Kikuchi (eds.), Balkema, Rotterdam.*
- Kohata, Y., Tatsuoka, F., Dong, J., Teachavorasinskun, S., Mizumoto, K., 1994. Stress states affecting elastic deformation moduli of geomaterials. *Proc. of Int. Symp. on Prefailure Deformation Characteristics of Geomaterials, IS-Hokkaido, '94, Balkema*, 1, 3-9.
- Kohata, Y., Tatsuoka, F., Wang, L., Jiang, G.L., Hoque, E., Kodaka, T., 1997. Modelling the non-linear deformation properties of stiff geomaterials, *Geotechnique* 47 (3), 563-580.
- Ortiz, M., Simo, J.C., 1986. An analysis of a new class of integration algorithms for elastoplastic constitutive relations. *International Journal of Numerical Methods in Engineering*, 23, 353-366.
- Siddiquee, M S.A. 1994. FEM Simulation of deformation and failure of stiff geomaterials based on element test results, Ph.D. Thesis, The University of Tokyo, Japan.
- Siddiquee, M.S.A., Tatsuoka, F., Hoque, E., Tsubouchi, T., Yoshida, O., Yamamoto, S., Tanaka, T. (1994). FEM simulation of footing settlement for stiff geomaterials, *Proc. of Int. Symposium Pre-Failure Deformation of Geomaterials (Shibuya et al., eds.), Balkema* 1, 531-537.
- Siddiquee, M.S.A., Tatsuoka, F., Kohata, Y., Yoshida, O. and Yamamoto, Y. and Tanaka, T., 1995. Settlement of a pier foundation for Akashi-Kaikyo Bridge and its numerical analysis, *Proc. Int. Workshop on Rock Foundation of Large Scale Structures, Tokyo, Balkema*, 413-420.
- Tanaka, T., Kawamoto, O., 1988. Three dimensional finite element collapse analysis for foundations and slopes using dynamic relaxation, *Proc. of Num. methods in geomechanics, Istanbul*, 1213-1218.
- Tatsuoka, F., Kohata, Y., 1995. Stiffness of hard soils and soft rocks in engineering applications, *Keynote Lecture, Proc. of Int. Symposium Pre-Failure Deformation of Geo-materials (Shibuya et al., eds.), Balkema*, 2, 947-1063.

- Tatsuoka. F., Kim,Y.-S., 1995. Deformation of shear zone in sedimentary soft rock observed in triaxial compression, Localisation and Bifurcation Theory for Soils and Rocks (Chambon et al., eds.), Balkema, 181-187.
- Tatsuoka.F., Lo Presti.D.C.F., Kohata.Y. 1995. Deformation characteristics of soils and soft rocks under monotonic and cyclic loads and their relationships. SOA Report, Proc. of the Third Int. Conf. on Recent Advances in Geotechnical Earthquake Engineering and Soil Dynamics. St Luis (Prakash eds.), 2, 851 -879.
- Yoshinaka, R., Yamabe, T., 1980. Strength criterion of rocks, Soils and Foundation, JSSMFE, 20 (4), 113-126.